Field and temperature-driven magnetic reversal of spin-flop coupled epitaxial Fe/MnPd bilayers

Wei Zhang* and Kannan M. Krishnan†

Department of Materials Science and Engineering, University of Washington, Seattle, Washington 98195, USA

(Received 31 March 2013; revised manuscript received 14 June 2013; published 30 July 2013)

We studied field and temperature-driven magnetic reversal of epitaxial spin-flop coupled Fe/MnPd bilayers. The onset temperatures for the spin-flop coupling, the loop shift, and the reversal asymmetry were found to be different for the same sample, indicating their sensitivity to different interface components. We show that the induced uniaxial anisotropy is a direct result of the spin-flop coupling, while the loop shift, observed along the bias, and the reversal asymmetry, measured perpendicular to the bias, are likely relevant to the local pinning environments and the remanence state of the ferromagnet. Further, the unidirectional bias can be manipulated by a controlled recooling process, while keeping the spin-flop property unaffected. Finally, we experimentally reveal the temperature-driven magnetization transitions in the thermal hysteresis of the bilayers and demonstrate the important role of competing energy terms on the observation of different types of thermal hysteresis behaviors.

DOI: 10.1103/PhysRevB.88.024428 PACS number(s): 75.70.Cn, 75.60.Jk, 75.30.Gw

I. INTRODUCTION

Exchange bias (EB) effect[1] in the ferromagnetic (F) and antiferromagnetic (AF) bilayers has attracted much interest for decades due to its wide applications in magnetoelectronic devices.[2] The key factor for EB is the AF spin behavior that contributes to the unidirectional anisotropy K_{eb}, causing the loop shift H_{eb}, and the induced uniaxial anisotropy K_u, being responsible for the coercivity enhancement.[3] In most cases, especially in polycrystalline samples, K_u is collinear with K_{eb}, hence distinguishing their contributions to the magnetic properties, including their specific effects on magnetic reversals, are not straightforward.[4,5] Existing models explaining the above effects usually assume an uncompensated AF surface, a collinear F/AF coupling at the interface, and two alternative behaviors of AF spins such that they are either pinned by anisotropy (contributing to the EB) or rotatable with the F magnetization (contributing to the enhanced coercivity).[2,6–8]

Despite a number of studies on the interesting individual spin behaviors, the various long-range effects, such as the lateral AF spin arrangement[9,10] and the AF bulk effect,[11–13] have not been fully investigated. Actually, such effects are quite critical, especially in epitaxial samples, where both structural coherence and magnetic ordering are optimized. For example, an orthogonal F/AF arrangement at the interface should be a natural consequence for a perfectly compensated AF surface regardless of the nature of F/AF coupling, since it minimizes the frustration of exchange coupling from the two AF sublattices.[14] Such *spin-flop* coupled systems are of great interest as they allow the evaluation of the long-range effects on the EB properties.[13] Additional higher-order anisotropies may arise, resulting in competing effects for magnetization reversal. In this sense, the spin-flop coupling has been demonstrated, both theoretically and experimentally, and interpreted in terms of an effective *uniaxial* anisotropy perpendicular to the field cooling (FC) direction;[14–18] however, it cannot explain the *unidirectional* bias effect,[15,18] and the loop shift observed in these systems should be attributed to interface effects other than the orthogonal coupling. Actually, random interface roughness for finite size domains would naturally lead to a unidirectional anisotropy, according to the well-accepted Malozemoff's theory.[19] In addition, other defects, such as dislocations, grain boundaries, and surface terraces, could also locally induce uncompensated regions that are oriented preferentially in the presence of the cooling field and thus break the symmetry.[15,17,20–22] As a result, the induced K_u is affected by the details of the exchange coupling at the interface, and K_{eb} is connected to other interface parameters, such as defects (natural and artificial), roughness,[23] and the cooling field. These different origins of the EB-induced uniaxial and unidirectional anisotropies also offer the possibility of studying, manipulating, and tailoring such effects independently.

In addition, the F magnetocrystalline anisotropy can be equally important, especially in single crystal samples, with the possibility of a higher-order symmetry such as fourfold.[24,25] The magnetic reversal is thus determined by the competing anisotropies induced from both interface and crystalline origins. An in-plane spin reorientation transition (SRT) of the ferromagnet may also occur due to the different behavior of the competing anisotropies as a function of temperature, film thickness, or the strength of exchange coupling.[26–28] This SRT has been theoretically predicted almost a decade ago;[26] however, it is only experimentally reported in a few cases.[18,29,30] In spite of the paucity of experiments, the correlation between the observed SRT properties and their origins at the interface needs to be established. A particularly interesting characteristic in such a SRT system is the thermal hysteresis,[31] in which the magnetization switching, from the reoriented state (RS) to the aligned state (AS) and vice versa, is driven by temperature. However, such an effect has been proposed only in theory and has not been experimentally observed so far.

Recently, Zhan *et al.* reported a low-temperature SRT in epitaxial Fe/MnPd bilayers, and in agreement with earlier theoretical predictions,[26,27] revealed that such SRT is driven by both the AF thickness and temperature.[32] Another recent work with x-ray imaging showed that such SRT can be also suppressed by the shape anisotropy induced from lithography patterning.[33] However, the temperature dependence of the induced anisotropies and their independent roles on the magnetic reversal has not been addressed. In this work, we have systematically studied the magnetic reversal of epitaxial Fe/MnPd

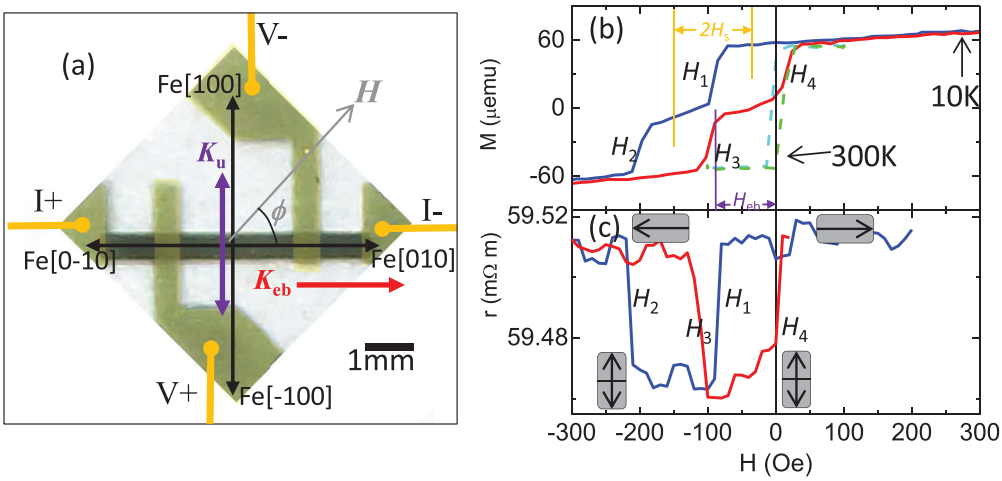

FIG. 1. (Color online) (a) Photograph of the sample (center stripe) and electrical contacts for AMR measurement. The relative orientations of the magnetic anisotropies, external field H, and the applied current I are indicated. (b) $M(H)$ curves measured along [010] at 300 K (dashed) and 10 K (solid) after FC from 300 K at $H_{FC} = 2$ kOe. (c) Corresponding $r(H)$ curve measured along [010] at 10 K after the same cooling process. The orientations of the Fe spins are represented by arrows enclosed in a rectangle.

bilayers over a wide range of temperatures. We observed different temperature behavior of the induced anisotropies, using vibrating sample magnetometry (VSM) and anisotropic magnetoresistance (AMR), which are equivalent methods for detecting field-driven magnetic reversals, by measuring magnetic switching from $M(H)$ and $r(H)$ curves, respectively. However, the AMR approach is advantageous over magnetometry due to its higher sensitivity to the magnetization distribution during the reversal process.[34–36] For instance, it is more accurate in determining successive two-step reversals and any possible intermediate states during the reversal,[34] which may be hard to distinguish from the $M(H)$ curves. In this work, we used AMR as much as possible to probe the magnetic reversal characteristics (Secs. III A and III B) but only used VSM when we studied the thermal hysteresis (Sec. III C) of the magnetization, $M(T)$. In Sec. III A, we show that the existence of EB can be uniquely confirmed if the following two characteristics are featured in the magnetic reversal: (1) the conventional loop shift observed along the bias direction; (2) an asymmetry in the magnetic reversal, favoring the bias direction along both descending and ascending branches of the hysteresis, when measured perpendicular to the bias. The existence of the unidirectional K_{eb} can be evidenced by the observation of either one of the above. In addition, the onset temperatures were different for the spin-flop coupling, the loop shift, and the reversal asymmetry. In Sec. III B, we demonstrate that the effects of K_{eb} and K_u on the magnetic reversal can be distinguished by controlled recooling process even below the blocking temperature T_B of the AF. Finally, in Sec. III C, we show experimental evidence for the thermal hysteresis in EB bilayers with SRT and demonstrate the important roles played by the competing energy terms on the different types of thermal hysteresis curves.

II. EXPERIMENTS

Epitaxial Fe (15-nm)/a axis MnPd (40-nm) bilayers in the shape of a 0.5-mm-wide stripe were deposited through a shadow mask on MgO(001) substrates by ion-beam sputtering following our earlier works[37,38] and specifically the recipe in Ref. 32. The Ta capping layer (5 nm) was used to prevent oxidation. Au contact pads, ~70 nm thick, were subsequently deposited for electrical measurements [Fig. 1(a)]. Magnetic properties were characterized using a physical property measurement system (PPMS, Quantum Design). Field hysteresis (loop) $M(H)$ and thermal hysteresis $M(T)$ were measured over the temperature range from 10 to 300 K by the standard VSM option of the PPMS; resistivity curves $r(H)$ were measured over the same temperature range by the resistivity option. A conventional four-point geometry was used for the AMR measurement, with the dc current I applied along Fe[010], an easy direction of the F anisotropy. In Fig. 1(a), an in-plane rotator was used to achieve different orientations, ϕ, of the in-plane magnetic field with respect to [010].

III. RESULTS AND DISCUSSIONS

Previous work has shown that the induced K_u reorients from parallel to perpendicular orientation with respect to the K_{eb} [Fig. 1(a)], once it is field cooled below T_B~95 K, of the a axis MnPd.[32] Figure 1(b) showed the hysteresis loop measured at 300 K (dashed), and at 10 K (solid) after cooling from 300 K in a cooling field, $H_{FC} = 2$ kOe along [010]. At 300 K, the small coercivity, ~7 Oe, indicates the small reversal barrier of the Fe layer alone. At 10 K, when K_{eb} and K_u are both established, a two-step, shifted loop was observed along [010]. The intermediate states, at H_1 along the descending branch and at H_3 along the ascending branch, indicate the magnetization aligned along K_u, i.e., [100] and/or [−100], established by the spin-flop coupling. The shift field, H_s, is determined from the center shift of the two subloops [Fig. 1(b)], i.e., $H_s = (H_1 - H_2 - H_3 + H_4)/4$, which is further related to K_u via $K_u = M_s H_s$, where M_s is the saturation magnetization. H_{eb} is determined by the center shift of the entire loop, i.e., $H_{eb} = |(H_1 + H_2 + H_3 + H_4)/4|$.

Figure 1(c) show the corresponding AMR curve at 10 K. The AMR originates from the anisotropic spin-orbit coupling effect that results in a resistance maximum when the magnetization is aligned along the direction of the current and a minimum when they are mutually orthogonal. The critical fields at which the magnetoresistance switches from a high to a low value (or vice versa) corresponds exactly to the switching fields observed in the hysteresis loop [Fig. 1(b)]. In this sense, $M(H)$ and $r(H)$ are equivalent methods for measuring the magnetic reversal, but the latter can be readily probed taking advantage of its higher sensitivity and resolution, plus the ability of applying the field along different directions by using the special sample rotator with the resistivity option of PPMS.

A. Temperature-dependent magnetization reversal

AMR was measured at the two perpendicular Fe easy directions, i.e., [010] ($\phi = 0^\circ$) and [100] ($\phi = 90^\circ$), respectively, after initial FC from 300 to 10 K at $H_{FC} = 2$ kOe parallel to [010]. Training effect was removed by large field (2 kOe) cycling prior to measurements. At 10 K, $r(H)$ measured along [010] showed a negative shift due to the strong K_{eb} along the same direction [Fig. 2(a)]. The intermediate, low-resistance state, as discussed above, indicates the magnetization reorientation along the perpendicular K_u. The establishment of EB upon different H_{FC} was first examined. To our surprise, almost the same magnitude of H_{eb} and H_s were induced at any value of a positive H_{FC}, including $H_{FC} = 0$ but approached from a finite positive field [dashed curve in Fig. 2(a)]. If we switch the sign of H_{FC} (including $H_{FC} = 0$ but approached from a finite negative field), a positive shift of $r(H)$ with the same magnitude of H_{eb} and H_s is observed (not shown). The FC-independent effect implies that the remanence of Fe magnetization, stabilized along the cubic easy axis by the anisotropy barrier, is sufficient to induce both EB and spin-flop coupling once cooled below T_B. The superficial need for the H_{FC} used for the EB is similar to the recent report on the crystallography-driven EB effect[39] and are both unique features of the single-crystal samples due to their strong magnetocrystalline anisotropy.

For the measurement along [100], the positive ([100]) and negative ([−100]) saturations both give rise to low-resistance states [Fig. 2(e)]. Suppose there is no unidirectional K_{eb} along [010]; the magnetization would switch directly from [100] to [−100] and vice versa, as dictated by the large K_u, without any intermediate state.[40,41] However, the observation of the intermediate, high-resistance state in the experiment indicates that the magnetization is aligned along [010], given by the K_{eb} during the reversal, for both descending and ascending branches. In other words, all magnetic reversals take place within the right semicircle that encloses the bias direction (inset Fig. 2(e)]. In practice, this is the other criterion for judging an exchange biased sample, especially when the loop shift is not obvious along the bias direction. Samples should be considered biased regardless of the loop shift, as long as such an intermediate state is observed with the field applied perpendicular to the bias. The magnitude of such unidirectional anisotropy, in the form of an effective field, K_{eb}/M_s, can be estimated by the separation of the two subloops, $K_{eb}/M_s = (H_5 - H_6 - H_7 + H_8)/4$ and can be a different value from the H_{eb} obtained along the bias direction.

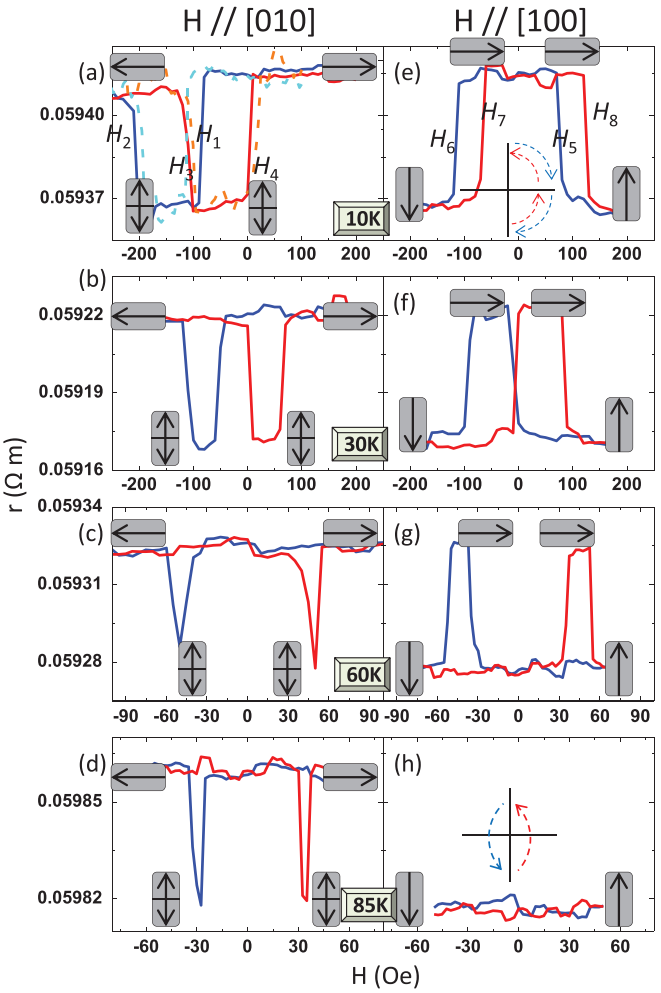

FIG. 2. (Color online) $r(H)$ curves measured along [010] at selective temperatures at (a) 10 K, (b) 30 K, (c) 60 K, and (d) 85 K, and along [100] at the same temperatures at (e) 10 K, (f) 30 K, (g) 60 K, and (h) 85 K, after the initial FC from 300 to 10 K at $H_{FC} = 2$ kOe. Dashed curve in (a) shows the $r(H)$ measured along [010] at 10 K after the initial cooling from 300 to 10 K at $H_{FC} = 0$ (but approached from a positive field). The orientations of the Fe spins are represented by arrows enclosed in a rectangle.

Similar $r(H)$ curves were measured at different temperatures up to 100 K in steps of 5 K during warming up (Fig. 2). In general, $r(H)$ along [010], shown by the left panel of Fig. 2, helps to determine H_{eb} and K_u/M_s, while $r(H)$ along [100], shown by the right panel of Fig. 2, allows to determine K_{eb}/M_s. For instance, $r(H)$ measured at 60 K along [010] is symmetrical around $H = 0$, i.e., $H_{eb} = 0$ [Fig. 2(c)]. However, the intermediate low- and high-resistance states can be still observed along [010] and [100], respectively, indicating finite values of both K_u and K_{eb} [Figs. 2(c) and 2(g)]. In other words, a unidirectional anisotropy is still present even if there is no observable EB field. At 85 K, the intermediate, high-resistance state [Fig. 2(h)] disappears along [100], but the intermediate, low-resistance state still exists along [010], which indicate a zero K_{eb} but a finite K_u [Fig. 2(d)]. The observation of a constant low-resistance state along [100] is due to the direct

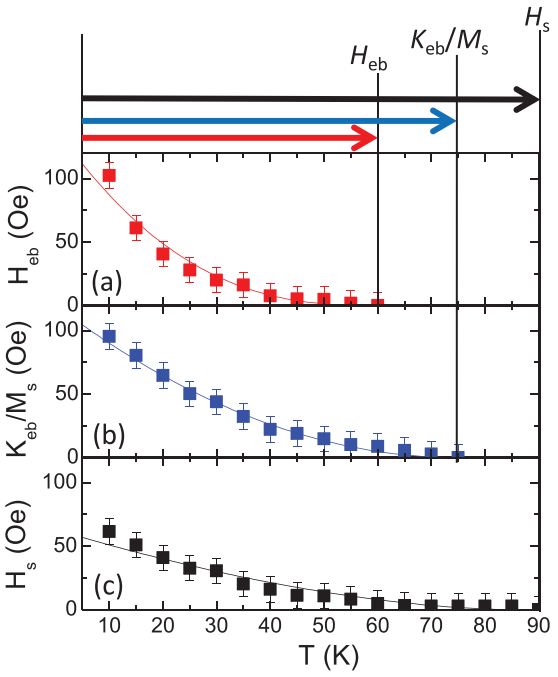

FIG. 3. (Color online) Temperature dependence (symbol) and corresponding fitting (curve) by the Malozemoff model of (a) loop shift, H_{eb}, (b) unidirectional anisotropy, K_{eb}/M_s, and (c) uniaxial anisotropy, K_u.

magnetic reversal from [100] to [−100] and vice versa when K_{eb} vanishes to zero [Fig. 2(h)].

Following the above discussions, H_{eb}, H_s, and K_{eb}/M_s can be obtained from $r(H)$ along [010] and [100] at each measuring temperature. Their temperature dependences are further summarized in Fig. 3. We found that the onset temperatures of the three parameters are different. The curve shift H_{eb} vanishes to zero at 60 K [Fig. 3(a)], but the intermediate state (symbolizing the presence of K_u) can be persistently observed until 90 K [Fig. 3(c)]. On the other hand, $r(H)$ data along [100] showed that the unidirectional anisotropy field, K_{eb}/M_s, derived from the reversal asymmetry, can persist up to 75 K [Fig. 3(b)].

Although the three parameters are simultaneously derived from the magnetization reversal, they can be distinct measures of the different interface components, because the microscopic spin structure in the bilayer is changed during the external field sweep as in magnetic reversal measurement. It is likely that the frozen-in states may be changed or destroyed leading to negligible unidirectional but non-negligible uniaxial (higher-order) anisotropy contributions, especially at temperatures close to T_B. Similar scenarios have been reported in collinear systems.[8,42,43] By using x-ray magnetic dichroism, it was shown that both the unidirectional reversal characteristic and higher-order anisotropies can be present without the observation of the loop shift.[8,44]

Different from the collinear-coupled case, the K_u in our sample is a direct result of the spin-flop coupling, and it can be persistently measured up to T_B of the MnPd layer, ∼95 K by magnetic reversal. Above T_B, the interface frustration by the two AF sublattices disappears (so does the spin-flop coupling), resulting in the simultaneous vanishing of K_u. On the other hand, the determination of H_{eb} and K_{eb}/M_s are both sensitive to the uncompensated characteristics at the interface, which may be independent of the spin-flop coupling. However, the different onsets of H_{eb} and K_{eb}/M_s indicate that the loop shift from magnetization reversal is not an accurate measure of the unidirectional anisotropy of the sample, but rather the reversal asymmetry is. Such reversal asymmetry is usually absent in collinear-coupled systems due to the lack of the distinct intermediate state during reversal. Only with x-ray magnetic dichroism, Ohldag *et al.*[42] showed that the AF spins in collinearly coupled Co/FeF_2 can rotate with the F moment ($H_{eb} = 0$), yet the anisotropy direction is still determined by the AF lattice ($K_{eb}/M_s \neq 0$). Here, by using simple magnetic reversal on a spin-flop system, we directly distinguished H_{eb} and K_{eb}/M_s and showed that the temperature onset for the reversal asymmetry is higher than that for the loop shift, yet both are manifestations of the unidirectional bias effect. The true blocking of the EB in this sample should be at 75 K, where all the unidirectional characteristics vanish completely.

In addition to the different sensitivity of K_u, H_{eb}, and K_{eb}/M_s to the magnetization reversal, it is also necessary to discuss their possible interface origins. As mentioned earlier, K_u can be directly explained by the spin-flop coupling. However, the necessary reversal pinning for explaining H_{eb} and K_{eb}/M_s is missing if a perfectly compensated interface is present.[45] H_{eb} and K_{eb}/M_s are thus related to interface uncompensation caused by roughness, defects, surface terraces, or antiphase boundaries.[17,19,46] The independent origin of unidirectional anisotropy is also supported experimentally by the simple fact that realistic negative,[32] positive,[18] and zero bias[47] have all been observed in spin-flop systems. The different signs of the bias can be attributed to local uncompensation spins plus the nature of F/AF coupling at the interface, i.e., either F (negative bias) or AF (positive bias). To further explore the different interface origins, we fitted the $H_s(T)$, $H_{eb}(T)$, and $K_{eb}/M_s(T)$ with the Malozemoff model,[19,48] i.e., $H_{eff}(T) = H_{eff}(0) \times (1 - T/T_{cri})^{\gamma}$, where H_{eff} is substituted with H_{eb}, K_{eb}/M_s, and H_s, with $T_{cri} = 60$, 75, and 90 K, respectively. The key parameter γ is a measure of the AF ordering, where $\gamma = 1$ indicates perfect cubic AF anisotropy.[49,50] The fitted γ for H_{eb}, K_{eb}/M_s, and H_s are 2.6, 2.0, and 1.7, respectively. Both H_{eb} and K_{eb}/M_s shows quite significant deviation from the case of cubic AF anisotropy, indicating that they are relatively independent with the long-range spin arrangements at the interface. However, H_s shows a smaller deviation as it results from the spin-flop coupling due to the interfacial long-range ordering. As a result, although the Malozemoff thoery is not an ideal model for our spin-flop bilayers, it provides a qualitative measure for the different interface origins of the uniaxial anisotropy and the unidirectional anisotropy. Such differences in origin further give rise to the possibility of separating their contributions in the magnetic reversal, as will be discussed in the next section.

B. Separation of the H_{eb} and H_s

The different interface origins of the EB-induced anisotropies further enable the independent manipulation of H_{eb} and H_s by controlled FC experiments. At any temperatures below T_B, resetting the cooling field does not affect K_u because

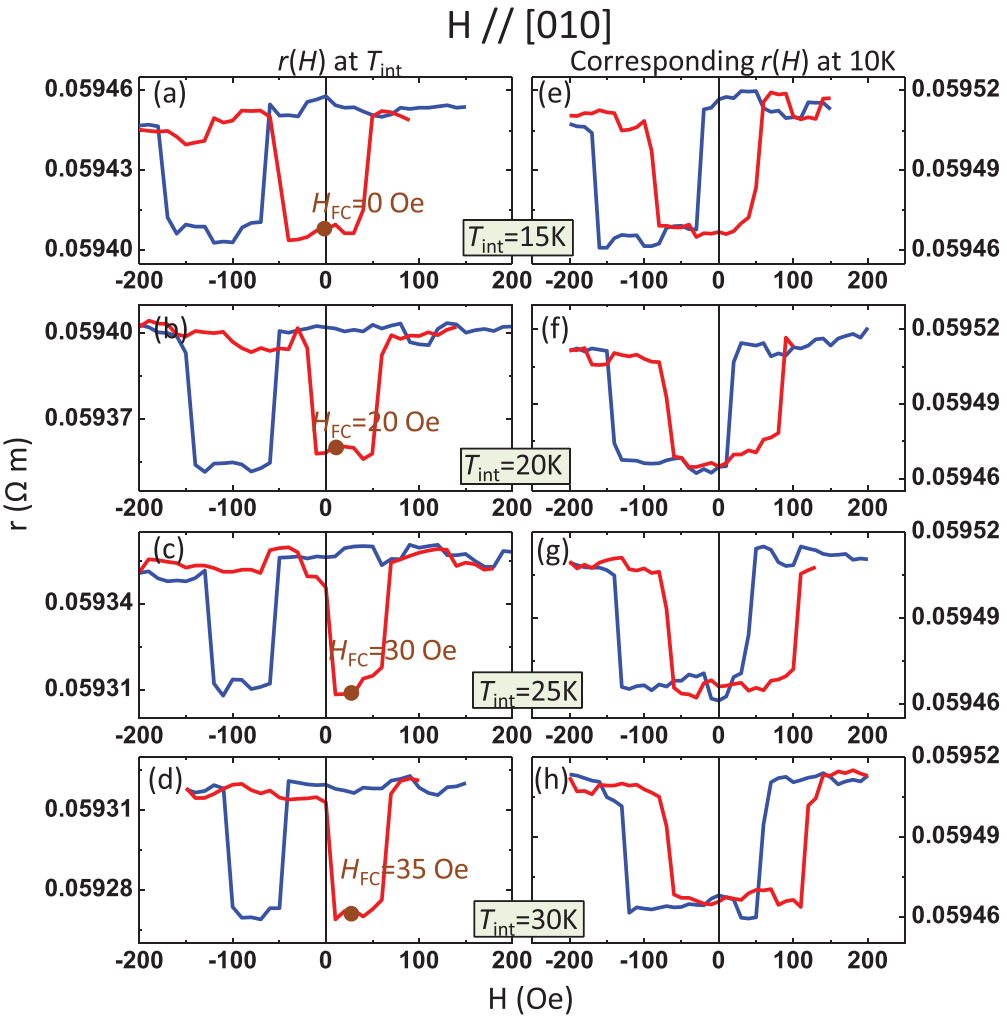

FIG. 4. (Color online) $r(H)$ curves measured along [010] at selective T_{int} (left panel), (a) 15 K, (b) 20 K, (c) 25 K, and (d) 30 K, after initial FC from 300 to 10 K at $H_{\text{FC}} = 2$ kOe, and their corresponding $r(H)$ curves measured at 10 K (e)–(h), after the recooling process from T_{int} under the new H_{FC} (value indicated in each figure of the left panel).

the intrinsic spin-flop coupling is frozen in. However, H_{eb} is sensitive to the local pinning environment, which can be altered (at least partially) by resetting the cooling field even below T_B. Figure 4 illustrates such a recooling process at four different $T_{\text{int}} = 15$, 20, 25, and 30 K. The sample is initially cooled from 300 to 10 K at $H_{\text{FC}} = 2$ kOe along [010] and then heated up to T_{int}, at which an $r(H)$ curve is measured (left panel in Fig. 4). Second, without altering the direction of H_{FC}, the strength of H_{FC} is fixed at a select value that stabilizes the magnetization along K_u (low-resistance state), taking advantage of the intrinsic SRT. We point out that different H_{FC} are used for different T_{int}. Next, the sample is cooled to 10 K under this new H_{FC}, and the $r(H)$ curve is measured again (right panel in Fig. 4). When compared to the initial $r(H)$ at 10 K [Fig. 2(a)], all the new $r(H)$ curves show a reduced H_{eb} and a slightly enhanced H_s. For $T_{\text{int}} = 30$ K, $r(H)$ measured after this particular recooling process is almost symmetrical with $H = 0$ [Fig. 4(h)], implying the erasing of H_{eb} along [010].

The underlying mechanism for such independent manipulation of H_{eb} is the redistribution of the pinning directions from primarily [010] to [100] and [−100] through the above recooling process. It relies on two facts: (1) the local pinning effects have lower thermal stabilities and therefore can be reset at T_{int} ($<T_B$); (2) the resultant K_{eb} can be efficiently set/reset just by the remanence of the F magnetization without using appreciable H_{FC} as discussed in Sec. III A. Here, the direction of H_{FC} is kept unchanged along [010] during recooling from T_{int} to 10 K; thus, an almost equal amount of pinning is expected to be induced along [100] and [−100] without changing the symmetry of the system. Such increased pinning along both ends of K_u leads to the slight enhancement of H_s. As a result, using such controlled recooling processes, we can tune the value of H_{eb} at low temperatures from its maximum to zero, while keeping the value of H_s and the symmetry of the system nearly unchanged. Finally, we want to point out that such tuning may be also achieved by directly applying a new H_{FC} along another direction (such as [100] and [−100]) at T_{int} to reorient the Fe magnetization, instead of using the intrinsic SRT. However, such a method will simultaneously develop a new unidirectional bias along the new H_{FC} and break the existing symmetry of the system.

C. Thermal hysteresis

Thermal hysteresis, although not new for magnetic multilayers,[51–54] has been only theoretically proposed in EB bilayers exhibiting the SRT, where the magnetic reversal from the RS to the AS (and vice versa) is expected to take place upon temperature increase/decrease, under competing magnetic energies.[31] The pioneering theoretical work showed the competing effect between the strong, induced K_u and the tunable Zeeman energy on the temperature-driven reversals.[31] Two types of thermal behavior have been proposed in distinct cases under low and high Zeeman energies, respectively. This theoretical frame is probably sufficient when dealing with Fe/FeF_2 system,[18] as the spin-flop coupling induces a strong K_u at the Fe-FeF_2 interface and a much weaker K_{eb}. However in our Fe/MnPd bilayers, a comparable K_{eb} also exists (in addition to K_u) that acts essentially as a temperature-dependent *effective field* on the sample. Depending on the relative orientation, such an effective field can either add on or cancel out the external applied field. This further complicates the system, especially when the temperature onset and dependence are different for K_{eb} and K_u. Finally, the temperature-driven F layer reversal at $T > T_B$ also needs to be considered. Figure 5 summarizes all the possible temperature-driven reversals in a Fe/MnPd bilayer: starting from the RS, i.e., [100], for example, the magnetization first switches to the AS([010]) upon heating driven by the strong K_{eb}, even though a constant external field, H_m, might be present along [0-10]. This is reflected by an increase of M in the $M(T)$ curve. At this point, if the sample is cooled back to low temperature, the magnetization will hold along [010] due to the reestablishment of the K_{eb} (type-I in Fig. 5). This behavior is of potential interest for magnetoelectronic applications in that a switch from an initial magnetic state to another final state is produced upon one temperature cycle. However, if the temperature further increases, K_{eb} will varnish, and the magnetization is continuously held along [010] by the Fe anisotropy barrier. Since the Fe anisotropy also decays with increasing temperature, eventually the external field can overcome the Fe barrier and the magnetic reversal occurs (type-II in Fig. 5). If the sample is then cooled to low temperature, a negative K_{eb} will establish and hold the magnetization along [0-10]. The transition point for [010] → [0-10] depends on the temperature behavior of K_{eb} and the Fe barrier, as well as the value of the external field. If a sufficiently large external field is present, the transition may occur at the beginning of the measurement, where a decrease of M in the $M(T)$ curve is observed (type-III in Fig. 5). As a result, it is the nonintermittent competition between the temperature-dependent K_{eb} and the constant external field that drives the temperature-driven magnetic reversal. Finally, if the two parameters exactly cancel out, another alternative scenario in which the magnetization is constantly held along RS by the single effective K_u can also happen. In this case, no temperature-driven reversal will be observed throughout the temperature sweeping (type-IV in Fig. 5).

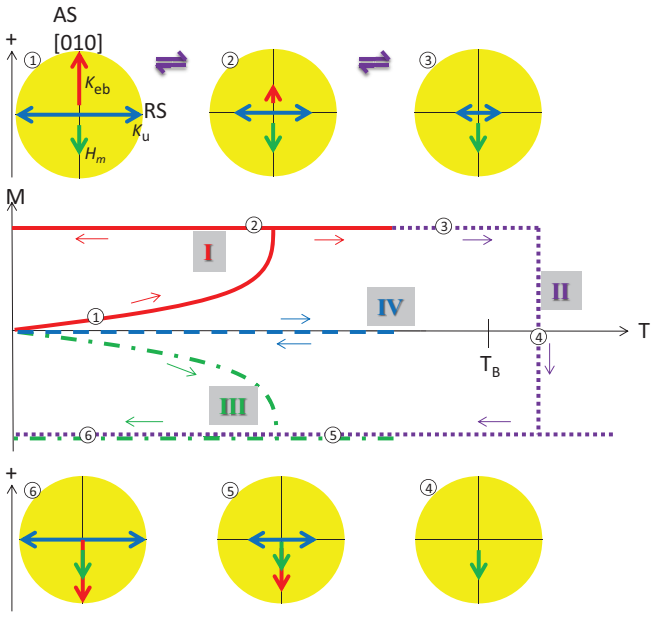

FIG. 5. (Color online) Illustration of the temperature-driven magnetic reversals and the different types of thermal behaviors in Fe/MnPd bilayers. Starting from RS, the magnetization reorients to [010] (type-I) or [0-10] (type-III) for a dominant K_{eb} or H_m, respectively. Since K_{eb} is temperature dependent, it is possible that the reversal is first governed by K_{eb} at low temperatures but then taken over by H_m at high temperatures (type-II). If K_{eb} and H_m are compensated, the system is dominated by the single K_u; therefore, no reversal occurs throughout the temperature sweep (type-IV). The relative anisotropy strengths at selective temperatures (1–6) are also illustrated.

We studied such temperature-driven reversals in our Fe/MnPd EB bilayers. First, the hysteresis loop is measured at 10 K [Fig. 6(a), middle panel] after FC from 300 K at $H_{FC} = 2$ kOe along [010]. Second, without changing the direction of H_{FC}, its strength is fixed at a select value, H_m, that aligns the magnetization along the perpendicular RS in the ascending branch. H_m is indicated, in the middle panel of Fig. 6(a), by a solid dot on top of the loop. In previous theoretical work, a small, positive H_m is usually good enough to stabilize the RS at low temperatures owing to the strong, induced perpendicular K_u.[31] However in our sample, a strong K_{eb}, in addition to K_u, is also induced, which is virtually equivalent to an effective field along [010]. Hence, negative values of H_m, which partly cancels the K_{eb}, need to be used to initialize the RS at 10 K in our case. With the field being fixed at H_m, a thermal hysteresis curve, $M(T)$, is then measured on heating the sample to 300 K (ascending) and cooling it to 10 K (descending).

Figures 6(b)–6(f) show different $M(T)$ curves at selective H_m. $M(T)$ at $H_m = -10$ Oe [Fig. 6(b)] exhibits a typical type-II behavior. Starting from the RS, a transition to the AS ([010]) is induced in the heating curve at T_1, by the effective field along the same direction given by the sum, $H_{eb}(T) + H_m$. The magnetization stays at [010] over a certain temperature range that even exceeds the T_B, after which the magnetization along AS is continuously held by the Fe anisotropy against the negative H_m. When temperature further increases, the Fe coercivity eventually becomes smaller than the applied, negative H_m, so the magnetization switches to the opposite AS ([0-10]) at T_2. During the cooling curve, a new EB along [0-10] is established by the F remnant magnetization along the same direction. Therefore, a positively shifted, stepped hysteresis loop is observed when cooled to 10 K [lower panel in Fig. 6(a)].

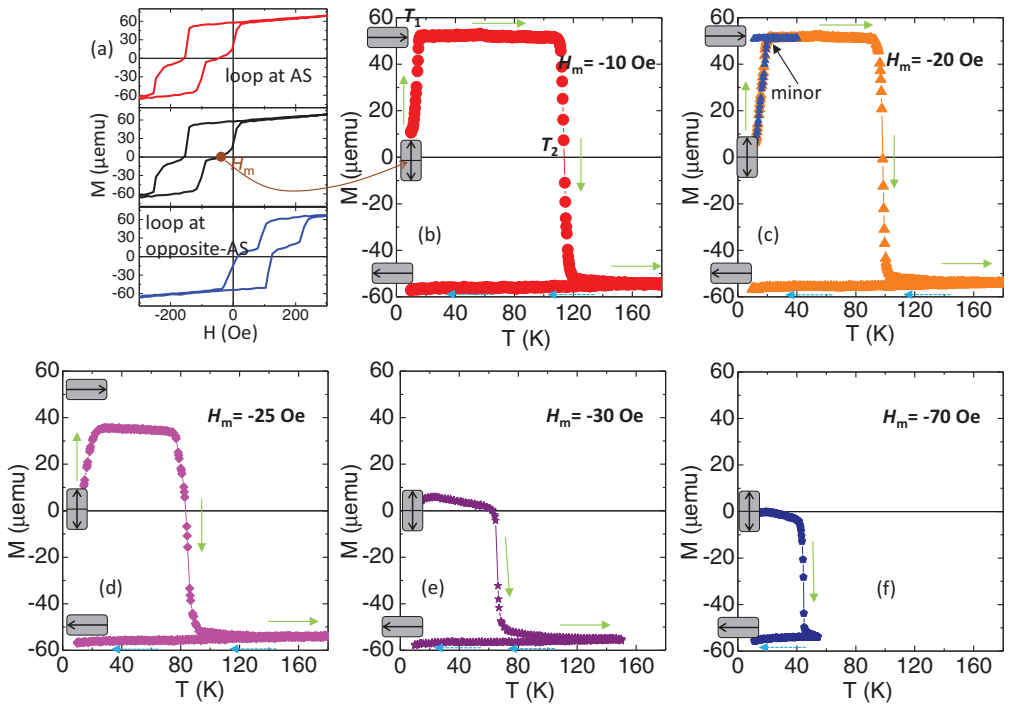

FIG. 6. (Color online) (a) Illustration of $M(H)$ characteristics at 10 K for initial state (middle panel), AS (upper panel), and opposite AS (lower panel). The field used to stabilize the RS, H_m, is also indicated in the initial loop. $M(T)$ curves measured at selective H_m (b) -10 Oe, (c) -20 Oe, (d) -25 Oe, (e) -30 Oe, and (f) -70 Oe, all starting from the RS. The minor curve for $H_m = -20$ Oe is also indicated. In each $M(T)$ curve, the orientation of Fe spins is represented by an arrow enclosed in a rectangle. The solid and dashed arrows indicate the heating and cooling branches, respectively.

Similar thermal behavior with two transitions at T_1 and T_2 can be observed for -30 Oe $< H_m \leqslant -10$ Oe. In all these cases, the magnetization begins from the initial RS, goes through an intermediate AS([010]) and finally ends up at the opposite AS ([0-10]) during a complete thermal cycle. Notably, the magnetization can return to AS ([010]) if subject to a minor thermal hysteresis, i.e., heating and measuring from 10 K to any T between T_1 and T_2, and cooling to 10 K (type-I). This is experimentally illustrated by the minor curve at $H_m = -20$ Oe [Fig. 6(c)]. Subsequently, the hysteresis loop measured at 10 K shows the conventional negative bias [upper panel in Fig. 6(a)].

Both the RS (stabilized by K_u) and the loop shift (induced by K_{eb}) originate at the interface and point to certain exchange energies, which are proportional to the thermal average value of the AF spins at the interface. Since the interface exchange energy vanishes at sufficiently high temperature, a transition in the heating branch is certain to occur. However, whether the magnetization transitions to [010] or to [0-10] depends on the effective field, $H_{eb}(T) + H_m$. For example, larger negative values of H_m ($\leqslant -30$ Oe) actually favor [0-10] (type-III) instead of [010] for the initial transition from RS and maintain such a state for the rest of the thermal cycle [Figs. 6(e) and 6(f)].

As mentioned above, a nontrivial, negative H_m is used to compensate K_{eb} and initialize the RS state. Such compensation is not maintained throughout the temperature sweep, since K_{eb} eventually vanishes at increasing temperatures. However, in Sec. III B, we showed that the K_{eb} can be independently manipulated by the specific recooling process. As a result, it is possible to study the temperature-driven reversal after appropriately erasing the K_{eb} along [010]. For example, after the initial FC from 300 to 10 K at $H_{FC} = 2$ kOe along [010], the sample is heated to $T_{int} = 30$ K and subsequently cooled to 10 K, at a reduced $H_{FC} = 40$ Oe (still along [010]) that reorients the Fe magnetization along K_u. The hysteresis loop at 10 K after the recooling exhibits nearly no loop shift ($H_{eb} \sim 0$), as shown by the middle panel in Fig. 7(a). Next, $M(T)$ curves were measured at selective H_m [Figs. 7(b)–7(f)]. Without the unidirectional K_{eb}, the transition is simply driven by H_m alone and thus favors AS ([010]) and opposite AS ([0-10]) when positive and negative H_m are used, respectively. Specifically, when a positive H_m is applied, it not only drives the transition from RS to AS but also maintains such a state during the cooling curve [Figs. 7(b) and 7(c)]. Similarly, the negative H_m drives the transition from RS to opposite AS and maintains such a state during the cooling curve [Fig. 7(f)]. As a result, the observed curves are primarily type-I or type-III, with only one transition observed over the whole temperature cycle.

We note that the measurement at exactly zero H_m [Fig. 7(e)] also exhibits a transition to opposite AS ([0-10]), which may be due to the imperfect erasing of the H_{eb} during the recooling experiment (negative effective field). This small residue of H_{eb} can be balanced by applying a comparable H_m with opposite sign to completely get rid of the effective pinning field along the [010] direction. On top of this assumption, if this H_m is also smaller than the Fe coercivity up to 300 K, the switching to other states above T_B can be prevented as well. In reality, we observed such a situation at $H_m = 5$ Oe [Fig. 7(d)], where the magnetization favors transitions along neither [010] nor [0-10], but preferably stays along the RS over the whole temperature

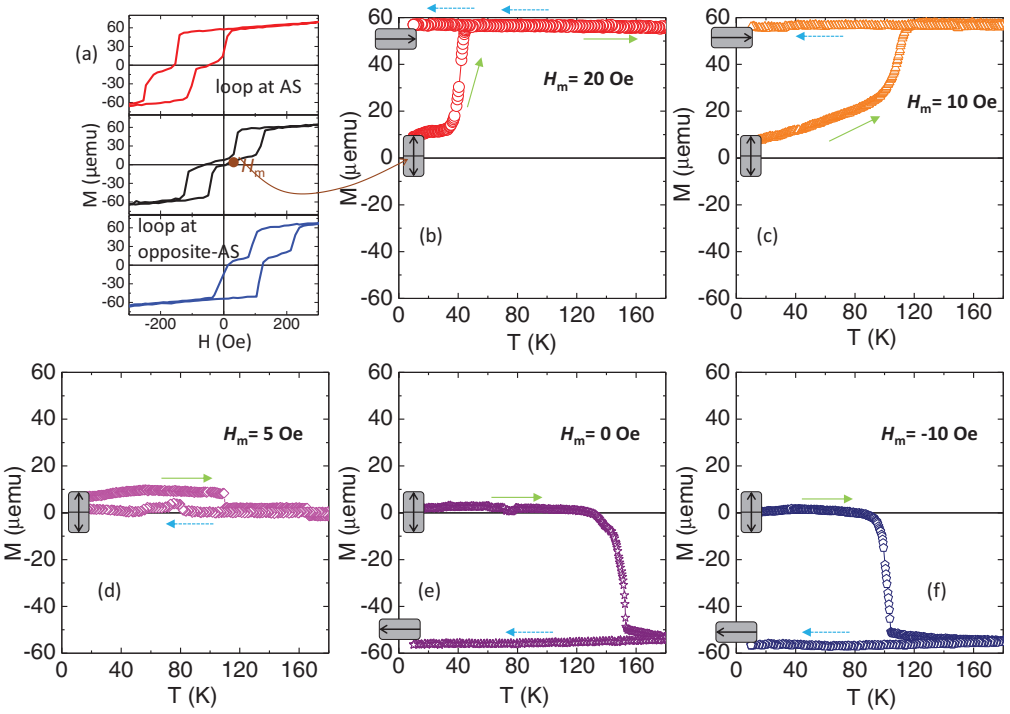

FIG. 7. (Color online) (a) Illustration of $M(H)$ characteristics at 10 K for initial state after the recooling process from 30 to 10 K at $H_{FC} =$ 40 Oe (middle panel), AS (upper panel), and opposite AS (lower panel). The field used to stabilize the RS, H_m, is also indicated in the initial loop. $M(T)$ curves measured at selective H_m (b) 20 Oe, (c) 10 Oe, (d) 5 Oe, (e) 0 Oe, and (f) −10 Oe, all starting from the RS. In each $M(T)$ curve, the orientation of Fe spins is represented by an arrow enclosed in a rectangle. The solid and dashed arrows indicate the heating and cooling branches, respectively.

cycle (type-IV). As a result, when the K_{eb} along [010] is properly balanced, the RS is stabilized by the perpendicular K_u up to T_B and then by the Fe reversal barrier, i.e., 7 Oe ($>H_m$) at 300 K, up to the maximum temperature (300 K) used in the measurement.

IV. CONCLUSION

In summary, we have carefully characterized the magnetic reversal properties in epitaxial Fe/MnPd bilayers exhibiting SRT. The existence of EB is characterized by two features in the magnetic reversal, i.e., the conventional loop shift observed along the bias direction and the reversal asymmetry measured perpendicular to the bias. Further, the different onset temperatures for the spin-flop coupling, the loop shift, and the reversal asymmetry indicate their sensitivity to different interface components. The induced K_u is a direct result of the spin-flop coupling, while H_{eb} and the reversal asymmetry are more relevant to the local pinning environments and the remanent state of the ferromagnet. In addition, we showed that the unidirectional bias can be independently manipulated by a controlled recooling process, while keeping the spin-flop property unaffected.

We also showed experimental evidence for the thermal hysteresis in EB bilayers exhibiting SRT. On the heating branch, we observed two distinct transitions, below and above T_B, which are driven primarily by the interface exchange energy and the Zeeman energy, respectively. The first transition is determined by the effective field along AS and can favor two opposite directions (AS and opposite AS) at different effective fields. The second transition is driven by the competition between the external field and the reversal barrier of the ferromagnet. On the cooling curve, the new EB established by the F remnant magnetization can prohibit the transition back to the RS at low temperatures. However, once the bias is erased (by the recooling experiment), the transitions are determined primarily by the external field, i.e., the transition simply favors AS and opposite AS when positive and negative fields are used, respectively. Moreover, if the external field is sufficiently small, i.e., less than the reversal barrier, the magnetization is constantly stabilized along the RS over the whole temperature cycle.

ACKNOWLEDGMENTS

This work was supported by NSF-DMR under Grant No. 1063489.

*Present address: Argonne National Laboratory, Lemont, IL 60439, USA; zwei@anl.gov
†Corresponding author: kannanmk@uw.edu

[1]W. H. Meiklejohn and C. P. Bean, Phys. Rev. **102**, 1413 (1956).
[2]See reviews: J. Nogués and I. K. Schuller, J. Magn. Magn. Mater. **192**, 203 (1999); A. E. Berkowitz and K. Takano, *ibid.* **200**,

552 (1999); M. Kiwi, *ibid.* **234**, 584 (2001); K. O'Grady, L. E. Fernandez-Outon, and G. Vallejo-Fernandez, *ibid.* **322**, 883 (2010); R. L. Stamps, J. Phys. D **33**, R247 (2000).
[3]T. Ambrose, R. L. Sommer, and C. L. Chien, Phys. Rev. B **56**, 83 (1997).
[4]J. Camarero, J. Sort, A. Hoffmann, J. M. Garcia-Martin, B. Dieny, R. Miranda, and J. Nogues, Phys. Rev. Lett. **95**, 057204 (2005).
[5]B. Beckmann, U. Nowak, and K. D. Usadel, Phys. Rev. Lett. **91**, 187201 (2003).
[6]S. Roy, M. R. Fitzsimmons, S. Park, M. Dorn, O. Petracic, Igor V. Roshchin, Zhi-Pan Li, X. Batlle, R. Morales, A. Misra, X. Zhang, K. Chesnel, J. B. Kortright, S. K. Sinha, and Ivan K. Schuller, Phys. Rev. Lett. **95**, 047201 (2005).
[7]S. Brück, G. Schütz, E. Goering, X. Ji, and K. M. Krishnan, Phys. Rev. Lett. **101**, 126402 (2008); S. Brück, S. Macke, E. Goering, X. Ji, Q. Zhan, and K. M. Krishnan, Phys. Rev. B **81**, 134414 (2010).
[8]J. Wu, J. S. Park, W. Kim, E. Arenholz, M. Liberati, A. Scholl, Y. Z. Wu, Chanyong Hwang, and Z. Q. Qiu, Phys. Rev. Lett. **104**, 217204 (2010).
[9]F. Radu, M. Etzkorn, R. Siebrecht, T. Schmitte, K. Westerholt, and H. Zabel, Phys. Rev. B **67**, 134409 (2003).
[10]F. Radu, S. K. Mishra, I. Zizak, A. I. Erko, H. A. Dürr, W. Eberhardt, G. Nowak, S. Buschhorn, H. Zabel, K. Zhernenkov, M. Wolff, D. Schmitz, E. Schierle, E. Dudzik, and R. Feyerherm, Phys. Rev. B **79**, 184425 (2009).
[11]R. Morales, Z. P. Li, J. Olamit, K. Liu, J. M. Alameda, and I. K. Schuller, Phys. Rev. Lett. **102**, 097201 (2009).
[12]F. Y. Yang and C. L. Chien, Phys. Rev. Lett. **85**, 2597 (2000).
[13]W. Zhang and K. M. Krishnan, Phys. Rev. B **86**, 054415 (2012).
[14]N. C. Koon, Phys. Rev. Lett. **78**, 4865 (1997).
[15]T. C. Schulthess and W. H. Butler, Phys. Rev. Lett. **81**, 4516 (1998).
[16]Y. Ijiri, J. A. Borchers, R. W. Erwin, S.-H. Lee, P. J. van der Zaag, and R. M. Wolf, Phys. Rev. Lett. **80**, 608 (1998).
[17]Y. Ijiri, T. C. Schulthess, J. A. Borchers, P. J. van der Zaag, and R. W. Erwin, Phys. Rev. Lett. **99**, 147201 (2007).
[18]T. J. Moran, J. Nogués, D. Lederman, and I. K. Schuller, Appl. Phys. Lett. **72**, 617 (1998).
[19]A. P. Malozemoff, Phys. Rev. B **35**, 3679 (1987).
[20]M. R. Ghadimi, B. Beschoten, and G. Güntherodt, Appl. Phys. Lett. **87**, 261903 (2005).
[21]K. Takano, R. H. Kodama, A. E. Berkowitz, W. Cao, and G. Thomas, Phys. Rev. Lett. **79**, 1130 (1997).
[22]I. Schmid, P. Kappenberger, O. Hellwig, M. J. Carey, E. E. Fullerton, and H. J. Hug, Europhys. Lett. **81**, 17001 (2008).
[23]J. Santamaria, M. E. Gómez, J. L. Vicent, K. M. Krishnan, and Ivan K. Schuller, Phys. Rev. Lett. **89**, 190601 (2002).
[24]W. Zhang, M. E. Bowden, and K. M. Krishnan, Appl. Phys. Lett. **98**, 092503 (2011).
[25]W. Zhang and K. M. Krishnan, J. Magn. Magn. Mater. **324**, 3129 (2012).
[26]P. J. Jensen and H. Dreyssé, Phys. Rev. B **66**, 220407(R) (2002).
[27]M. L. Silva, A. L. Dantas, and A. S. Carriço, J. Magn. Magn. Mater. **292**, 453 (2005).
[28]J. H. Seok, H. Y. Kwon, S. S. Hong, Y. Z. Wu, Z. Q. Qiu, and C. Won, Phys. Rev. B **80**, 174407 (2009).
[29]E. J. Escorcia-Aparicio, Hyuk J. Choi, W. L. Ling, R. K. Kawakami, and Z. Q. Qiu, Phys. Rev. Lett. **81**, 2144 (1998).
[30]J. Li, M. Przybylski, F. Yildiz, X. L. Fu, and Y. Z. Wu, Phys. Rev. B **83**, 094436 (2011).
[31]F. I. F. Nascimento, A. L. Dantas, L. L. Oliveira, V. D. Mello, R. E. Camley, and A. S. Carriço, Phys. Rev. B **80**, 144407 (2009).
[32]Q. F. Zhan and K. M. Krishnan, Appl. Phys. Lett. **96**, 112506 (2010).
[33]E. Folven, A. Scholl, A. Young, S. T. Retterer, J. E. Boschker, T. Tybell, Y. Takamura, and J. K. Grepstad, Nano Lett. **12**, 2386 (2012).
[34]W. Zhang and K. M. Krishnan, J. Appl. Phys. **111**, 07D712 (2012).
[35]M. Klaui, C. A. F. Vaz, J. Rothman, J. A. C. Bland, W. Wernsdorfer, G. Faini, and E. Cambril, Phys. Rev. Lett. **90**, 097202 (2003).
[36]S. Brems, K. Temst, and C. Van Haesendonck, Phys. Rev. Lett. **99**, 067201 (2007).
[37]N. Cheng, J.-P. Ahn, and K. M. Krishnan, J. Appl. Phys. **89**, 6597 (2001).
[38]P. Blomqvist, K. M. Krishnan, and D. E. McCready, J. Appl. Phys. **95**, 8019 (2004).
[39]A. K. Suszka, O. Idigoras, E. Nikulina, A. Chuvilin, and A. Berger, Phys. Rev. Lett. **109**, 177205 (2012).
[40]R. P. Cowburn, S. J. Gray, and J. A. C. Bland, Phys. Rev. Lett. **79**, 4018 (1997).
[41]Q. F. Zhan, S. Vandezande, K. Temst, and C. Van Haesendonck, Phys. Rev. B **80**, 094416 (2009).
[42]H. Ohldag, H. Shi, E. Arenholz, J. Stohr, and D. Lederman, Phys. Rev. Lett. **96**, 027203 (2006).
[43]W. N. Cao, J. Li, G. Chen, J. Zhu, C. R. Hu, and Y. Z. Wu, Appl. Phys. Lett. **98**, 262506 (2011).
[44]J. Li, Y. Meng, J. S. Park, C. A. Jenkins, E. Arenholz, A. Scholl, A. Tan, H. Son, H. W. Zhao, C. Hwang, Y. Z. Wu, and Z. Q. Qiu, Phys. Rev. B **84**, 094447 (2011).
[45]N. J. Gökemeijer, R. L. Penn, D. R. Veblen, and C. L. Chien, Phys. Rev. B **63**, 174422 (2001).
[46]Q. F. Zhan, W. Zhang, and K. M. Krishnan, Phys. Rev. B **83**, 094404 (2011).
[47]M. R. Fitzsimmons, C. Leighton, J. Nogués, A. Hoffmann, K. Liu, C. F. Majkrzak, J. A. Dura, J. R. Groves, R. W. Springer, P. N. Arendt, V. Leiner, H. Lauter, and I. K. Schuller, Phys. Rev. B **65**, 134436 (2002).
[48]A. P. Malozemoff, J. Appl. Phys. **63**, 3874 (1988).
[49]N. N. Phuoc and T. Suzuki, IEEE Trans. Magn. **43**, 897 (2007).
[50]W. Zhang, D. N. Weiss, and K. M. Krishnan, J. Appl. Phys. **107**, 09D724 (2010).
[51]S. Demirtas, M. R. Hossu, R. E. Camley, H. C. Mireles, and A. R. Koymen, Phys. Rev. B **72**, 184433 (2005).
[52]R. E. Camley, W. Lohstrohb, G. P. Felcherc, N. Hosoitod, and H. Hashizume, J. Magn. Magn. Mater. **286**, 65 (2005).
[53]M. R. Hossu, Y. Hao, and A. R. Koymen, J. Phys.: Condens. Matter **20**, 215224 (2008).
[54]J. P. Andrés, J. A. González, T. P. A. Hase, B. K. Tanner, and J. M. Riveiro, Phys. Rev. B **77**, 144407 (2008).